

Simulation of Tidal Fields around a Huge Floating Marina using a Multi-level Method

SUNG YOUN BOO*

*Dept. of naval Architecture, Korea Naval Academy, Jinhae, Korea

KEY WORDS: Tidal circulation, Multi-level model, Floating marina, Residual current, Volume flux, Velocity field, Density field

ABSTRACT: Floating marina has been interests as an alternative to the facilities for recreational boats because of its cost effectiveness and less environmental conflicts. For the present research, a square floating marina with a length of 400m and draft of 5m was used. This marina can be extended to 800m by putting another one together. Tidal field around the marina was simulated using a multi-level finite difference method. Tidal motion was assumed sinusoidal in a closed rectangular bay. Velocities and residual current were investigated for two cases of single marina and two marinas installed in the bay. It was found that the horizontal velocity fields from the water surface to the structure bottom around the marina were affected. In the marina basin, magnitude of velocity was reduced considerably but overall quality of water circulation was preserved even after two marinas were installed.

1. Introduction

Utilization of coastal zone as an alternative to the land-based airports has brought great concerns because of less environmental conflict and better accessibility of airplane to the landing spot. A floating airport (Inoue et al., 1994) is a typical example of a structure installed in bay.

A marina to keep the yachts, motorboats and supplies has usually been constructed in harbor. However, environmental problem can arise from sediments, waste water and circulation loss in this land-based marina since it is constructed in a harbor with narrow entrance to protect the boats from waves. Some coastal-based marina sites can, thus, be chosen in order to use enough tidal flushing. One of the potential maria for this purpose is a floating type structure.

Even though the floating marina can reduce the water pollution, water quality around the marina site can be dependent on the size and draft of the maria and location installed. It is also known that water quality in basin depends on retention time of tide, flushing rate, velocity fields or mixing process.

The mathematical hydrodynamic model based on the three-dimensional shallow water equation can be treated various way. A multi-level finite difference method is well implemented in Falconer (1990), Fusino and Tabeta (1993), Inoue et al. (1994) and Boo (1999).

Finite element hydrodynamic model, for instance, Chen et al. (1991), Kodama et al. (1996) in which complex geometries can be efficiently represented with proper mesh distributions, is also applied to the shallow water problem.

A multi-level finite difference model of TIDS3dTS (Boo, 1997) was employed to simulate the tidal flow circulation around a very large floating structure located in a bay. For the present research, the model has been upgraded further.

A square floating marina with a length of 400m and breadth of 5m, was assumed to be placed in a rectangular closed bay. This maria was also extended to 800m by putting two marinas side by side. The single as well as two marina structures were used in simulating the tidal fields.

Tidal motion at the inlet was assumed sinusoidal. Velocities and residual currents were compared for the two different cases. In addition, volume flux rate was also examined after installation of the marinas.

2. Basic Equations

Assuming hydrostatic pressure distribution, which is valid when the vertical acceleration is negligible compared to the vertical pressure gradient, and applying the Boussinesq approximation, the governing equations of continuity and momentum for incompressible fluid flow in a cartesian coordinate system with the z -axis directed vertically upwards are:

$$\frac{\partial u}{\partial x} + \frac{\partial v}{\partial y} + \frac{\partial w}{\partial z} = 0 \quad (1)$$

* 제1저자 부성윤 연락처: 경남 진해시 우체국 사서함 88호
055-549-1263 syboo@navy.ac.kr

$$\frac{Du}{Dt} = -\frac{1}{\rho_o} \frac{\partial p}{\partial x} + fv + E_h \left(\frac{\partial^2 u}{\partial x^2} + \frac{\partial^2 u}{\partial y^2} \right) + E_v \frac{\partial^2 u}{\partial z^2} \quad (2)$$

$$\frac{Dv}{Dt} = -\frac{1}{\rho_o} \frac{\partial p}{\partial x} - fu + E_h \left(\frac{\partial^2 v}{\partial x^2} + \frac{\partial^2 v}{\partial y^2} \right) + E_v \frac{\partial^2 v}{\partial z^2} \quad (3)$$

$$\frac{1}{\rho} \frac{\partial p}{\partial z} + g = 0 \quad (4)$$

where $\frac{D}{Dt} = u \frac{\partial}{\partial x} + v \frac{\partial}{\partial y} + w \frac{\partial}{\partial z}$; u , v and w are velocity components in the x , y and z directions; f is the Coriolis force parameter calculated by $2\Omega \sin \phi$, Ω the rotational angular velocity of the earth and ϕ the latitude; ρ_o a constant reference density of fluid; ρ the density of sea water; E_h the horizontal eddy viscosity coefficient; E_v the vertical eddy viscosity coefficient; p the water pressure; g the acceleration of gravity. Similarly, variation of water temperature T and salinity S can be written as:

$$\frac{DT}{Dt} = D_h \left(\frac{\partial^2 T}{\partial x^2} + \frac{\partial^2 T}{\partial y^2} \right) + D_v \frac{\partial^2 T}{\partial z^2} \quad (5)$$

$$\frac{DS}{Dt} = D_h \left(\frac{\partial^2 S}{\partial x^2} + \frac{\partial^2 S}{\partial y^2} \right) + D_v \frac{\partial^2 S}{\partial z^2} \quad (6)$$

where D_h and D_v are the horizontal and vertical eddy diffusive coefficients. The water density is assumed to be a function of temperature and salinity. It can be calculated from:

$$\rho(T, S) = 1028.152 - 0.0735T - 0.004691T^2 + (0.802 - 0.002T)(S - 35.0) \quad (7)$$

In eq. (2)-(3) and (5)-(6), the vertical eddy viscosity E_v and the diffusive coefficients D_v can be determined using

$$E_v = E_{v0} \times \frac{1}{(1 + 5.2R_i)}, \quad D_v = E_{v0} \times \frac{1}{(1 + 0.33R_i)} \quad (8)$$

where E_{v0} is the vertical eddy viscosity under homogeneous condition, and R_i is the Richardson number defined as:

$$R_i = -\frac{g}{\rho} \frac{\partial \rho}{\partial z} / \left(\left(\frac{\partial u}{\partial z} \right)^2 + \left(\frac{\partial v}{\partial z} \right)^2 \right) \quad (9)$$

3. Boundary Conditions

The boundary conditions for the velocity fields on the

free surface are represented as

$$\frac{\partial \zeta}{\partial t} + u \frac{\partial \zeta}{\partial x} + v \frac{\partial \zeta}{\partial y} - w = 0 \quad (10)$$

$$E_v \frac{\partial u}{\partial z} = \frac{\tau_{xu}}{\rho_o}, \quad E_v \frac{\partial v}{\partial z} = \frac{\tau_{yv}}{\rho_o} \quad (11)$$

$$\tau_{xu} = C_{10} \rho_a u_w \sqrt{u_w^2 + v_w^2}, \quad \tau_{yv} = C_{10} \rho_a v_w \sqrt{u_w^2 + v_w^2} \quad (12)$$

where ζ is the surface elevation; τ_{xu} and τ_{yv} are the wind shear stress in the x and y directions; u_w and v_w the velocity components in the $x-y$ plane; C_{10} is the air drag coefficient at the sea surface; ρ_a the air density. Additional boundary conditions for temperature and salinity on the free surface are described as:

$$E_v \frac{\partial T}{\partial z} = \frac{Q_T}{\rho_o C_p}, \quad E_v \frac{\partial S}{\partial z} = \frac{Q_S}{\rho_o} \quad (13)$$

where Q_T is the exchange rate of temperature per unit area and time between water surface and air; Q_S the exchange rate of salinity; C_p the specific heat. Bottom boundary conditions are written as:

$$u \frac{\partial h}{\partial x} + v \frac{\partial h}{\partial y} + w = 0 \quad (14)$$

$$E_v \frac{\partial u}{\partial z} = \frac{\tau_{xb}}{\rho_o}, \quad E_v \frac{\partial v}{\partial z} = \frac{\tau_{yb}}{\rho_o} \quad (15)$$

$$\tau_{xb} = \gamma \rho_a u_b \sqrt{u_b^2 + v_b^2}, \quad \tau_{yb} = \gamma \rho_a v_b \sqrt{u_b^2 + v_b^2} \quad (16)$$

where τ_{xb} and τ_{yb} are the bottom frictional shear stress in the x and y directions; u_b and v_b the velocity components at the bottom level; γ is the bottom frictional coefficient; h the water depth. It is assumed that no flux of temperature and salinity present through the sea bottom.

The tidal elevation at the open boundary is given in a harmonic function of eq. (17). Velocity gradient normal to the open boundary is assumed zero as well.

$$\zeta(x, y, t) = \zeta_o \sin \frac{2\pi}{T_o} t \quad (17)$$

where T_o and ζ_o are the period and amplitude of tide.

At the closed boundary of shore line, non-slip condition is imposed. Also, normal velocity to the boundary and

gradient of tidal elevation are set zero. It is also assumed that no flux of temperature and salinity occur. These conditions can be expressed as:

$$\vec{u} \cdot \vec{n} = 0, \frac{\partial T}{\partial \hat{n}} = \frac{\partial S}{\partial \hat{n}} = 0 \quad (18)$$

where \vec{u} and \vec{n} are the horizontal flow velocity vector and normal vector; \hat{n} is the normal direction to the closed boundary.

4. Modeling of Floating Structures

We can assume that there will be two different shapes of floating structures for the current research. One is a barge type structure which has considerable breadth (Fig. 1) and the other is a flat plate type structure of which thickness is negligible compared to the mesh size on the horizontal plane (Fig. 2). Therefore, an appropriate scheme must be introduced into the multi-level model in order to represent two different floating structures. This is described in the following sections.

4.1 Barge-type structure

It is assumed that an imaginary sea surface exists inside the structure and the imaginary elevation ζ , thus, changes along with the tidal elevation. The imaginary elevation inside the structure can be computed by interpolating the elevation data just out of the structure. For the convenience, we assume that the fluid domain under the structure is called "domain II", and others are called "domain I" as illustrated in Fig. 1.

The vertical momentum equation (4) can be integrated with respect to z :

$$p = p_a + \rho_a g(\zeta - z) + g \int_z^\zeta \rho' dz \quad (19)$$

where $\rho = \rho_a + \rho'$. Since eq. (19) is valid only in domain I, another scheme is required to compute the pressure in domain II. The equation (4) is integrated from the structure bottom d to the imaginary surface ζ . The resulting equation for the water pressure at the structure bottom in domain II is written as:

$$p_d = p_a + \rho_a gD \quad (20)$$

where $D = \zeta + d$. Also, eq. (4) can be further modified by integrating from the sea bottom to the structure bottom in

domain II and the resulting equation is:

$$p = p_d - \rho_a g(d + z) + g \int_z^d \rho' dz \quad (21)$$

Velocity and density fields conditions on the boundary of the structure are imposed using schemes similar to eq. (18).

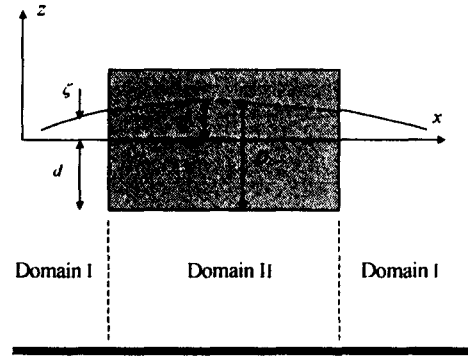


Fig. 1 Schematics of a barge type floating structure and imaginary tidal elevation

4.2 Flat plat type structure

Difference of the tidal elevation between two sides of the flat plate type structure can be assumed zero as long as the structure is afloat. This means that pressure can be computed with an assumption that the thin structure is transparent to the tidal wave (Fig. 2). The pressure equation (19) can, thus, be applicable in the entire fluid domain as if the structure does not present.

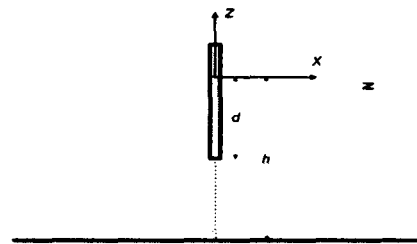


Fig. 2 Schematics of a flat plate type floating structure

However, the structure can affect velocity, thermal and salinity fields. This must, thus, be taken into account. Velocities normal to the structure are set zero while tangential velocities on it are allowed. In addition, since no flow exists crossing the structure, the convection and diffusion terms in eq. (5) and (6), normal to the surface, are given zero.

6. Numerical Results

Numerical test was carried out in a rectangular bay with length \times breadth \times depth=1800m \times 1400m \times 15m. The bay size was determined by taking into account the size of the floating marina used for the present work. The principal dimension of the marina was chosen as length \times breadth \times draft = 400m \times 400m \times 5m. It also consists of multi-blocks which can provide the internal basins, entrances, fairways and berth places. Length of the marina can be extended to 800m by putting another one side by side as shown in Fig. 3. East side of the bay was assumed to be an open boundary where a tidal forcing with an amplitude of 1.0m and period of 12 hours were given.

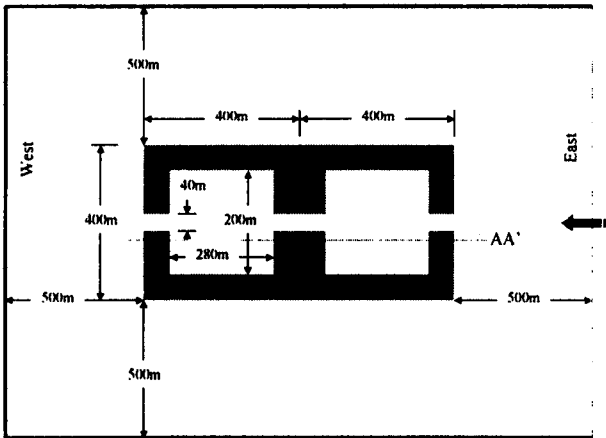


Fig. 3 Floating marina in the rectangular bay

Mesh sizes in the horizontal and vertical directions were properly chosen as 20m and 1m, respectively, in order to represent the structure shape. Distance between marinas to the shore was set to be 500m.

Numerical simulation was performed for three different cases. In Case 0, no structure was placed. In Case I, the single floating marina with 400m long was installed in the bay while in Case II, two marinas were used.

6.1 Velocity fields on the horizontal plane

Velocity fields at the maximum flood tide at the "level 1" which corresponds to the water surface of $z=0m$, are shown in Fig. 4 for Case I and in Fig. 5 for Case II. It can be seen that magnitude of velocity is reduced much in the marina basin for both cases. Also, surface velocities outside the structure including near the open boundary are generally larger when one marina is installed than when two marinas are used.

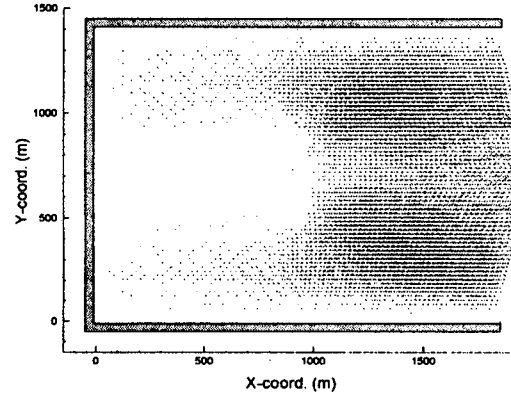


Fig. 4 Velocity at the maximum flood tide at level 1 ($z=0m$) for Case I

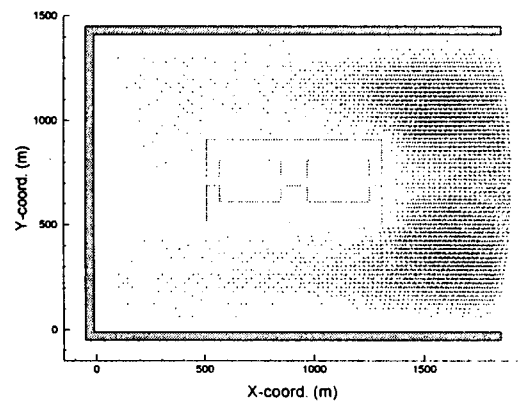


Fig. 5 Velocity at the maximum flood tide at level 1 ($z=0m$) for Case II

In order to investigate tidal fields under the water surface, "level 4" which is at $z=-3m$ was chosen. This location is in between the water surface and bottom of the floating marina. In Fig. 6 and 7, velocity fields for Case I and Case II at the "level 4" are illustrated. Flow circulation inside and outside the marina are very similar to those shown in Fig. 4 and 5 except the opposite direction of the flow.

6.2 Velocity fields on the vertical plane

Vertical distribution of the flow velocity along the center line of AA' shown in Fig. 3 is illustrated in Fig. 8 and 9. Horizontal velocity from the water surface to the bottom level of the structure is seen to be much reduced due to

the floating marina. It can also be seen that the horizontal velocities near the bottom level are greater than those near the water surface. This means that the velocity loss near the water surface are compensated by the increased velocity between the structure bottom and sea bottom. Thus, difference of total volume flux through the bay entrance before and after installation of the floating becomes small.

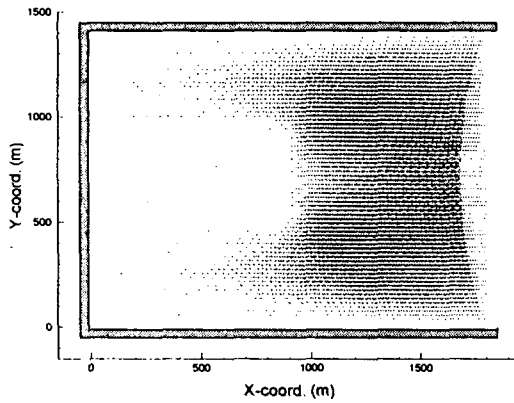


Fig. 6 Velocity at the maximum ebb tide at level 4 ($z = -3m$) for Case I

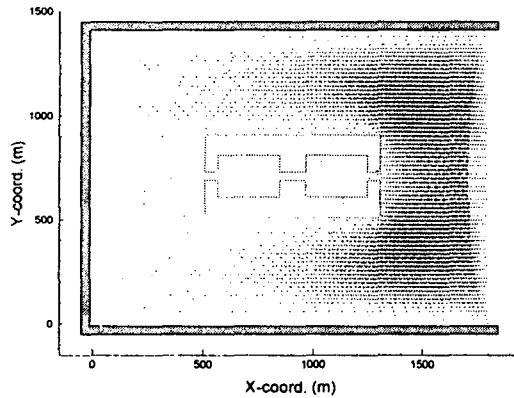


Fig. 7 Velocity at the maximum ebb tide at level 4 ($z = -3m$) for Case II

6.3 Residual Currents

Residual currents at the water surface are shown in Fig. 10 and 11. Flows in the marina basin is seen to be very small. Residual currents flowing toward the marina near the bay entrance are generated while, inside the bay, opposite currents flowing outward exist. Since these two opposite flows meet near the marina, nearly stagnant flow region is

formed.

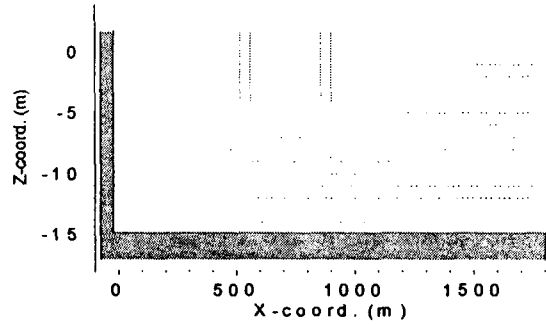


Fig. 8 Velocity along the line AA' of the bay at the maximum ebb tide for Case I

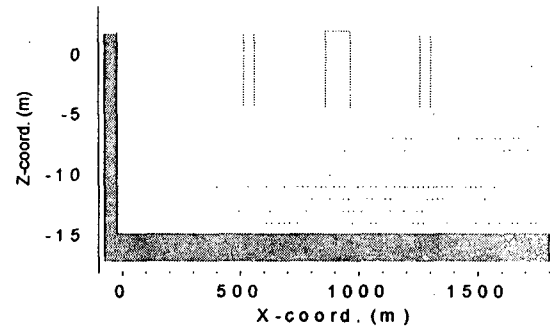


Fig. 9 Velocity along the line AA' of the bay at the maximum ebb tide for Case II

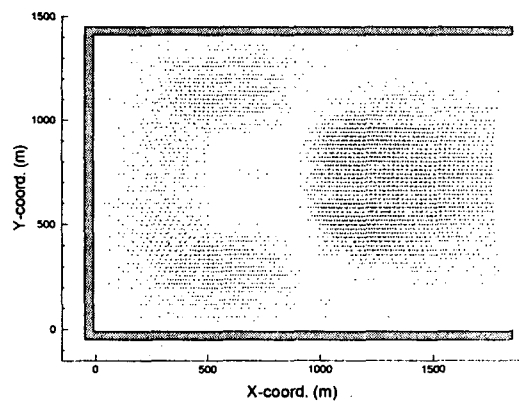


Fig. 10 Residual currents at level 1 ($z = 0m$) for Case I

6.4 Volume flux rate

Volume flux rate through the bay entrance may change after the marina is installed inside the bay. If the volume flux rate decreases considerably after installation, this can

cause an environmental problem near the structure. In Fig. 12, volume flux rates for Case 0, I and II are compared. Here, positive flux represents the flow from the bay entrance toward the bay inside. A negligible difference between Case 0 and Case I is found. In Case II, the volume flux decreases in an amount of 9.5% at the maximum flood (or ebb) tide, compared to the Case 0.

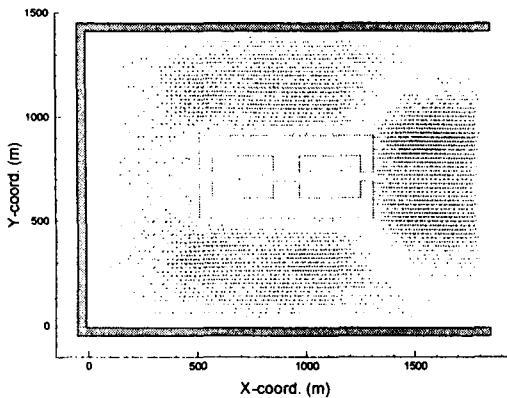


Fig. 11 Residual currents at level 1 ($z=0m$) for Case II

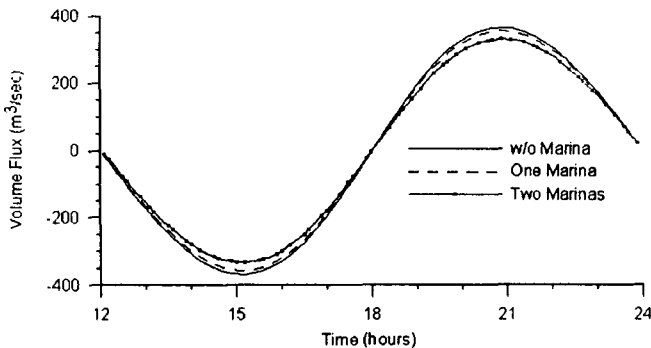


Fig. 12 Comparison of volume flux rates for Case 0, I, and II at the open boundary.

7. Conclusions

Coastal environment may be changed when a very large structure is installed in the bay. A floating structure is, thus, an alternative to facilities for various purposes. In this research, a floating marina for recreational boats was chosen and the flow fields after installation of it was simulated.

A square floating marina with a length of 400m and draft of 5m was used. This structure consists of multi-blocks which enable to provide the internal basins, entrances, fairways and berth places. This maria can also extended to

800m by putting another one side by side.

Tidal field computation around the floating structure was conducted using a multi-level finite difference method. Tidal motion was assumed sinusoidal in a closed rectangular bay. Velocities and residual currents were investigated for two cases of single marina and two marinas installed in the center of the bay. It was found that velocity fields around the marina was affected. Especially inside basin, the magnitude of velocity was reduced considerably but overall quality of tidal fields in the bay was preserved even after 800m-long marina was installed.

Further simulation may be required for various tidal environments as well as actual site where the marina will be installed.

References

- Boo, S. Y. (1999). "A Study on the Thermal Fields control using a Floating -type Current Control Structure", Journal of Ocena Engineering Technology, KCORE, Vol 13, No 2, pp 147-158 (in Korean).
- Boo, S. Y. (1997). "TIDE3dTS; 3-D Analysis Code of Tide, Temperature and Salinity Fields around a Lage Floating Structure", User's Manual, Final Report, KRISO, Daejon, Korea (in Korean).
- Chen, C.L. and Lee, K.K. (1991). "Great-Lakes River-Estuary Hydrodynamic Finite Element Method", J. Hydraulic Engineering, Vol. 117, No. 11.
- Falconer, R.A. (1990). "Numerical Modeling of Tidal Circulation in Harbors", J. Waterway, Port, Coastal and Ocean Division, Vol. 106, No. WW1.
- Inoue, Y., Tabeta, S., Arai, M. and Kazawa, K. (1994). "Feasibility Design of a Floating Airport and Investigation into its Effects on the Environment", Journal of the Society of Naval Architects of Japan, Vol. 176, pp 75-81.
- Kodama, T., Wang, S. and Kawahara, M. (1996) "Model Verification on 3D Tidal Current Analysis in Tokyo Bay", Intl. J. for Numerical Method in Fluid, Vol. 22.
- Tabeta, S. and Fusino, M. (1994). "Numerical Simulation of Currents and Density Variation in Tokyo Bay by means of Multi-Level Model", Journal of the Society of Naval Architects of Japan, Vol. 176, pp 67-74.

2004년 월 일 원고 접수

2004년 월 일 수정본 채택